

Empirical Analysis of Stability of $A_{n+1}B_nO_{3n+1}$ Ruddlesden–Popper Phases Using Reciprocal n -Values

Sergei Vereshchagin ^{1,*}  and Vyacheslav Dudnikov ² 

¹ Institute of Chemistry and Chemical Technology, Federal Research Center KSC SB RAS, Russian Academy of Sciences, Akademgorodok 50/24, 660036 Krasnoyarsk, Russia

² Kirensky Institute of Physics, Federal Research Center KSC SB RAS, Akademgorodok 50/38, 660036 Krasnoyarsk, Russia; slad63@yandex.ru

* Correspondence: snv@icct.ru

Abstract: Layered $A_{n+1}B_nO_{3n+1}$ ($n = 1 \dots \infty$) Ruddlesden–Popper (RP) phases are a promising system for a variety of applications. Within the RP family, the thermodynamic properties of the phases are essentially additive with variation in the n value, but at present, there are no general approaches that would allow one to evaluate the individual stability of the RP phases and the possibility of their interconversion. The aim of this paper is to present a novel concept for performing a thermodynamic analysis of RP phases using the reciprocal values of the index n . We present an empirical equation $\Delta G_{1/n} = \Delta G_P + B_1/n + B_2/n^2$, where $\Delta G_{1/n}$ and ΔG_P are the molar Gibbs energies of formation of the Ruddlesden–Popper (RP) phase $(AO)_{1/n}ABO_3$ and the parent ABO_3 perovskite, respectively, and n is a stoichiometry index of $A_{n+1}B_nO_{3n+1}$ RP phase. The correlation was validated using available thermodynamic data for the systems Sr–Ti–O, Ca–Ti–O, Sr–Zr–O, La–Ni–O, and La–Co–O. For all A–B combinations, the equation quantitatively describes the Gibbs energy of RP phase formation. Predicted values for the non-linear approximation lie within the experimental uncertainty in determining $\Delta G_{1/n}$. The proposed correlation was used to analyze the relative stability of the RP phases and to determine the feasibility of synthesizing new compounds.

Keywords: perovskites; Ruddlesden–Popper phases; Gibbs free energy; thermodynamics



Citation: Vereshchagin, S.; Dudnikov, V. Empirical Analysis of Stability of $A_{n+1}B_nO_{3n+1}$ Ruddlesden–Popper Phases Using Reciprocal n -Values. *Crystals* **2024**, *14*, 954. <https://doi.org/10.3390/cryst14110954>

Academic Editor: Andrei V. Shevelkov

Received: 15 October 2024

Revised: 30 October 2024

Accepted: 30 October 2024

Published: 31 October 2024



Copyright: © 2024 by the authors. Licensee MDPI, Basel, Switzerland. This article is an open access article distributed under the terms and conditions of the Creative Commons Attribution (CC BY) license (<https://creativecommons.org/licenses/by/4.0/>).

1. Introduction

Compounds with the ABO_3 composition and perovskite structure, as well as layered perovskite-like $A_{n+1}B_nO_{3n+1}$ Ruddlesden–Popper (RP) phases, are among the most attractive and interesting mixed oxides due to their outstanding functional properties [1]. In the last decade, RP phases based on rare earth oxides and transition metals Mn, Fe, and Co have attracted particular interest as functional materials for solid fuel elements [2,3], oxygen-permeable materials [4] and electrocatalysts as a single-phase [5,6] or perovskite-based composites [7].

$A_{n+1}B_nO_{3n+1}$ RP phases are a homologous series of layered substances which originate from perovskite ABO_3 . The structure of the n -th member of the RP family can be visualized as alternating AO layers with a rock salt structure, separated by n layers of ABO_3 with a perovskite structure. The stoichiometry of such phases is usually written as $A_{n+1}B_nO_{3n+1}$ or $AO(ABO_3)_n$ ($n = 1 \dots \infty$). Thus, the first member of the series is the compound A_2BO_4 ($n = 1$), and the last is perovskite ABO_3 ($n = \infty$).

A theoretical study of the electronic structure of $Sr_{n+1}Ti_nO_{3n+1}$ ($n = 1–3, \infty$) shows that with increasing index n , the $A_{n+1}B_nO_{3n+1}$ phases become unstable with respect to dissociation, the predicted limit of phase stability being $n \approx 3$ [8,9]. This is in line with experimental published data for Sr–Ti–O [10], Sr–Ru–O [11,12], Ca–Ti–O [13], La–Ni–O [14,15] series; compounds with $n = 1–3$ were fabricated using standard high-temperature methods of ceramic synthesis. Nevertheless, the high n members of the RP $Sr_{n+1}Ti_nO_{3n+1}$ family were prepared using molecular beam epitaxy and pulsed laser deposition methods for

$n = 4-6$ [16], $n = 1-5$ and 10 [17], or an unprecedented $n = 20$ RP phase, $\text{AO} \cdot (\text{ATiO}_3)_{20}$ ($A = \text{Ba}_{0.6}\text{Sr}_{0.4}$) [18].

An analysis of the literature has shown that, at present, very few studies have been published in which the thermodynamic properties of RP phases are systematized, making it possible to quantitatively predict their stability when the value of n changes. The thermodynamic properties of $\text{A}_{n+1}\text{B}_n\text{O}_{3n+1}$ ($n = 1-4, \infty$) compounds for Ca-Ti-O, Sr-Ti-O, Sr-Zr-O, Sr-Mo-O, and Sr-W-O systems have been analyzed to examine the stabilities of perovskites and RP phases [19]. The chemical potential diagrams (a $\log[a(A)/a(B)]$ vs. $\log P_{\text{O}_2}$) were constructed using a computer program and the available estimated or experimental thermodynamic data. A thermodynamic analysis was performed on the dissociation reaction of A_2MO_4 compounds into perovskites AMO_3 and alkaline earth oxides (AOs) using empirical correlations between stabilization energy and the tolerance factor. It was shown that the correlation between the tolerance factor and enthalpy of formation among perovskites was found to be very useful to predict an absence of some perovskite phase in certain systems. Thermodynamics of layered perovskites was systematically considered in [20]. Based on thermodynamic data for perovskites and RP phases of various chemical compositions, the paper demonstrates that thermodynamic layer values are substantially additive, thus permitting prediction of the properties for materials with unknown values. Similar conclusions were drawn in paper [21]. Based on dissolution enthalpies of $\text{La}_{n+1}\text{Ni}_n\text{O}_{3n+1}$ complex oxides, the thermochemical characteristics of these oxides from binary oxides were calculated. It was found that there is a linear dependence (1) between the enthalpy of formation of any complex oxide in the RP series and the value of n :

$$\Delta H = 30.9 - 971n \text{ (kJ/mol La)} \quad (1)$$

These approaches, based on the additivity of properties and their linear correlation with the n value, have two significant drawbacks. Firstly, strict additivity implies full reversibility of a transformation. For example, the reversibility of PR phase dissociation, Equation (2), results in a failure to synthesize a pure $\text{AO}(\text{ABO}_3)_n$ phase. Therefore, it is necessary to take into account deviations from linearity (additivity), the magnitude of which, despite their small values, will most likely determine the stability of the products.



Secondly, when analyzing the dependence $F = f(n)$, where F is any property and $n = 1 \dots \infty$, the ABO_3 perovskite ($n = \infty$) falls out of consideration.

In this paper, we consider a new approximation to describe the stability of RP phases using reciprocal values of index $1/n = 1, 1/2, 1/3 \dots 0$. The aim of the study is to formulate general relationships covering a wide range of RP phases and test these relations using published thermodynamic experimental data for different sets of A and B cations that can form layered perovskite-like phases.

2. Materials and Methods

Here, and below, the abbreviation RP_n is used for an n -th member of the Ruddlesden-Popper family ($\text{A}_{n+1}\text{B}_n\text{O}_{3n+1}$, $\text{AO} \cdot (\text{ABO}_3)_n$ or $(\text{AO})_{1/n} \cdot \text{ABO}_3$, $n = 1 \dots \infty$).

Gibbs energies of formation (ΔG_n) were used as a measure of RP_n phase stability. The thermodynamic quantities of the RP_n -forming systems ($n = 1-3, \infty$) were collected from the appropriate publications (Sr-Ti-O [19,22]; Ca-Ti-O [23]; Sr-Zr-O [19]; La-Ni-O [15]; La-Co-O [24,25]). Values of ΔG_n at 298 K were used without any transformation as they appear in the parent papers. High temperature values of ΔG_n were calculated for a reference temperature 1200 K using the equations given in the original sources. Values of ΔG_n for stoichiometry $\text{A}_{n+1}\text{B}_n\text{O}_{3n+1}$ were converted to the reciprocal scale $1/n$ (stoichiometry $(\text{AO})_{1/n} \cdot \text{ABO}_3$, $1/n = 1, 1/2, 1/3, 0$) using the obvious expression (3):

$$\Delta G_n(\text{A}_{n+1}\text{B}_n\text{O}_{3n+1}) = n \cdot \Delta G_{1/n}((\text{AO})_{1/n}\text{ABO}_3) \quad (3)$$

3. Results and Discussion

We will now construct the n -th member of the RP family by stacking n layers of perovskite on an AO layer. The work to create such a structure can be written as (4), and dividing both sides of the equation by n , we obtain (4a).

$$\Delta G_n = n\Delta G_P + \Delta G_{AO} \quad \text{for } \text{AO}(\text{ABO}_3)_n \text{ phase} \quad (4)$$

$$\Delta G_{1/n} = \Delta G_n/n = \Delta G_P + \Delta G_{AO}/n \quad \text{for } (\text{AO})_{1/n}\text{ABO}_3 \text{ phase} \quad (4a)$$

where ΔG_n , $\Delta G_{1/n}$ —molar Gibbs energies of $\text{AO}(\text{ABO}_3)_n$ and $(\text{AO})_{1/n}\text{ABO}_3$ formation, accordingly;

ΔG_P , ΔG_{AO} —increments corresponding to the addition of the perovskite or AO layer.

As a first approximation, let us assume that the values of ΔG_{AO} and ΔG_P do not depend on n . This means that the expression (4a) is valid for any n and that the value of $\Delta G_{1/n}$ (molar Gibbs energy of $(\text{AO})_{1/n}\text{ABO}_3$ formation) is a linear function of $1/n$ $\Delta G_{1/n} = A' + B_1'/n$. In this equation, A' (y-intercept) is equal to ΔG_P (the Gibbs energy of ABO_3 perovskite formation), since $\Delta G_{1/n} = \Delta G_P$ at $n = \infty$ and B_1' is a slope (empirical fitting parameter).

Using available thermodynamic data from [15,19,22–25], the values of $\Delta G_{1/n}$ were calculated for different A-B combinations, and the results were plotted against $1/n$ (Figure 1a). It can be seen that the experimental points for all systems satisfactorily correspond to the linear dependence; for all cases, Pearson product-moment correlation coefficients were found to be not less than 0.998. Figure 1b shows the approximation of the points for $(\text{SrO})_{1/n}\text{SrTiO}_3$ by a linear function (4a) in more detail; the residual plot for the regression of $\Delta G_{1/n}$ vs. $1/n$ is shown in Figure 1b, inset (red line). A pronounced non-random U-shaped pattern suggests a better fit for a non-linear model (5), where B_1' and B_2' are empirical fitting parameters. To assess correspondence of the linear (4a)/non-linear quadratic model (5) to the data, a successive F-test was employed to check whether the $1/n^2$ term results in a significant improvement. It shows that at a 0.05 significance level, model (5) is more likely to be correct ($F_{\text{exp}} = 1035.9 > F_{\text{crit}}(0.95,1,1) = 18.5$). It should be pointed out that in the case of $(\text{SrO})_{1/n}\text{SrTiO}_3$, predicted values for the non-linear approximation lie within the experimental uncertainty in determining $\Delta G_{1/n}$ and the same regularities are valid for the rest of the A-B cations under consideration (Figure 1a).

$$\Delta G_{1/n} = \Delta G_P + B_1'/n + B_2'/n^2 \quad (5)$$

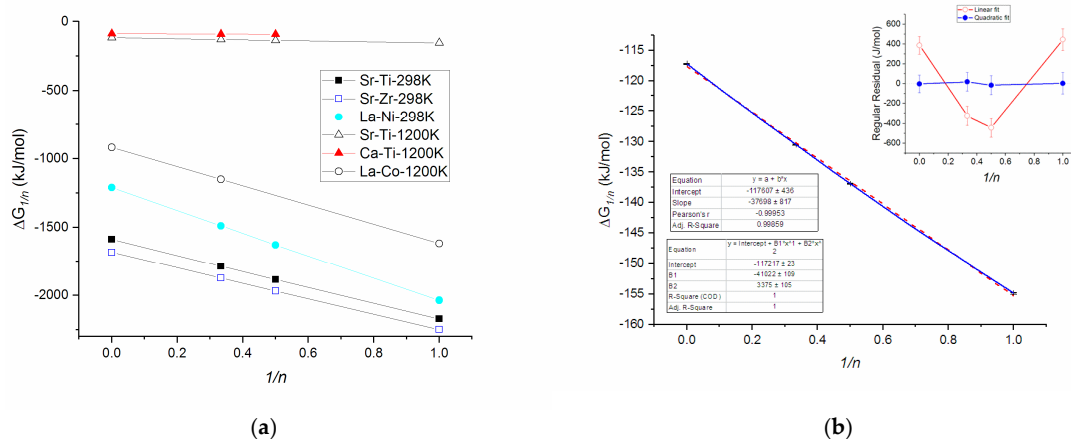
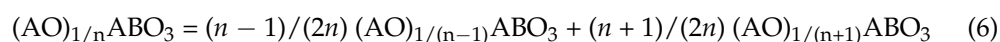


Figure 1. (a) Molar Gibbs energies of $(\text{AO})_{1/n}\text{ABO}_3$ formation ($\Delta G_{1/n}$) for various A-B combinations as a function of $1/n$; (b) Linear (dashed, red) and quadratic (solid, blue) approximation of $\Delta G_{1/n}$ as a function of $1/n$ for $(\text{SrO})_{1/n}\text{SrTiO}_3$. Inset: residual plot (observed-predicted) vs. $1/n$ for linear (open, red) and non-linear (closed, blue) regression models. The whiskers show the experimental uncertainties of $\Delta G_{1/n}$ taken from [22].

The existence of dependence (5) gives rise to a number of significant and unanticipated consequences.

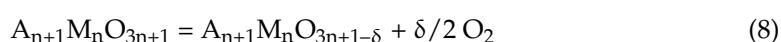
1. As follows from Figure 1b (inset), the accuracy of the approximation of $\Delta G_{1/n}$ by Equation (4) is higher than the uncertainty of its experimental determination. Thus, Equation (5) can be used to estimate the Gibbs energy of formation of any member of the RP family, which cannot be determined experimentally, and to verify the values obtained experimentally.
2. Let us consider the possibility of the disproportionation reaction of an RP_n phase into $RP(n-1)$ and $RP(n+1)$ phases by Equations (2) and (6):



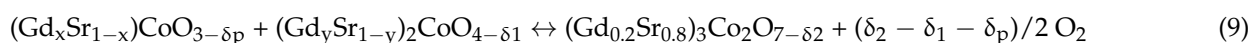
It is easy to show that the change in the Gibbs energy $\Delta G_{r,n}$ of reaction (6) is reduced to expression (7) if correlation (5) is valid. Given that $B'_2 > 0$ (Figure 1b), this means that for any $n > 1$, $\Delta G_{r,n}$ is positive. Therefore, there is no inherent instability of PR_n phases which was predicted in theoretical studies for $n \geq 3$ ([8,9]).

$$\Delta G_{r,n} = \frac{B'_2}{n^2(n^2 - 1)} \quad (7)$$

3. The absolute value of the change in the Gibbs free energy of reaction (6) of interconversion of the RP phases is small. In particular, in the case of strontium titanates, it does not exceed 281 J/mol at 1200 K. This is exactly what causes the difficulty of synthesizing the RP phases $A_{n+1}B_nO_{3n+1}$ with a high n value. On the other hand, low values of $\Delta G_{r,n}$ make it possible to influence the relative stability of the RP phases and, accordingly, to shift the equilibrium of their interconversion, using a factor that affects the thermodynamics of compounds with different n to varying extents. Oxygen non-stoichiometry, for instance, can act as such a factor for systems based on transition metals (Co, Ni, Fe). It is known that double perovskites $(AA')MO_3$ and the RP phases (A, A' = rare and alkaline earth metals, M = Co, Ni, Fe), are capable of reversibly adding/eliminating oxygen (8) to form non-stoichiometric compounds depending on the temperature and partial pressure of oxygen.



To date, it has not been possible to find systematic experimental data in the literature on the influence of oxygen non-stoichiometry δ on the thermodynamic quantities (enthalpy, entropy, Gibbs energy) of $A_{n+1}M_nO_{3n+1}$ compounds with different n values. Therefore, it is not possible to quantitatively confirm the assumption made. However, a qualitative illustration of the relationship between non-stoichiometry and stability of the RP phase with a certain value of the index n is the observation of the sequential disproportionation of perovskite $LaCoO_3$ to $La_4Co_3O_{10}$, La_2CoO_4 and CoO at 1100–1400 K with a decrease in the partial pressure of oxygen from 10^5 to 10^{-10} Pa [25]. It has also been suggested that direct decomposition of $La_3Ni_2O_{7-\delta}$ leads to the formation of $La_2NiO_{4-\delta}$ and $La_4Ni_3O_{10-\delta}$ under the process of electrochemical oxygen removal at 1400 K [26]. The formation and development of oxygen and ruthenium vacancies by adjusting the oxygen partial pressure was shown to facilitate a phase transition from $SrRuO_3$ to $Sr_3Ru_2O_7$ [27]. An additional indication of the validity of this assumption is the reversible interconversion (9) of the type $ABO_3 + A_2BO_4 \leftrightarrow A_3B_2O_7$ for the system $0.3 Gd_2O_3 - 1.2 SrO - CoO$, occurring at 1243–1473 K with oxygen pressure variations in the range from $2 \cdot 10^4$ to 1 Pa [28].



4. A further generalization of the approximation (5) can be obtained by reducing the equation to a dimensionless form (10), where $B_1 = B_1'/\Delta G_P$ and $B_2 = B_2'/\Delta G_P$.

$$G_{n/P} = (\Delta G_{1/n}/\Delta G_P - 1) = (\Delta G_{1/n} - \Delta G_P)/\Delta G_P = B_1/n + B_2/n^2 \quad (10)$$

This transformation allows us to describe the energetics of the RP phases in all A-B-O series based on a minimum number of empirical parameters. Figure 2 shows the experimental data transformed according to Equation (10); the lines are fitted experimental values of $(\Delta G_{1/n}/\Delta G_P - 1)$ to the reciprocal index n . Table 1 shows the estimates of parameter B_1 and B_2 which were obtained using a non-linear least squares estimation procedure. The dimensionless form (10) of Equation (5) represents the most complete generalization of the implicit dependence of the Gibbs energy of formation of a $A_{n+1}B_nO_{3n+1}$ member of the RP family on the index n . Transformation of the experimental points using Equation (10) results in a set of closely spaced curves passing through the origin, individual differences associated with the nature of the A and B cations being much less pronounced (Figures 1a and 2). Moreover, a comparison of the curves at 298 K and 1200 K for the $Sr_{n+1}Ti_nO_{3n+1}$ system (Figure 2; ■ and △ points) demonstrates that the influence of temperature is effectively neutralized.

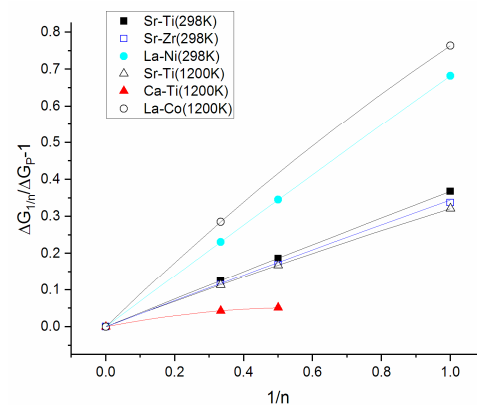


Figure 2. Comparing fitted (lines, Equation (10)) and experimental values of $(\Delta G_{1/n}/\Delta G_P - 1)$ as a function of the reciprocal index n .

Table 1. Number of $(AO)_{1/n}ABO_3$ phases (N) included in calculation (fitting), their indexes (n) and estimates of parameter B_1 and B_2 , Equation (10).

System	N	df	n	B_1	B_2
$Sr_{n+1}Ti_nO_{3n+1}$ (1200K)	4	2	1–3,∞	0.34985 ± 0.00046	-0.02873 ± 0.00051
$Ca_{n+1}Ti_nO_{3n+1}$ (1200K)	3	1	2,3,∞	$0.17996 \pm 1 \times 10^{-16} *$	$-0.15427 \pm 2 \times 10^{-16} *$
$La_{n+1}Co_nO_{3n+1}$ (1200K)	3	1	1,3,∞	$0.90318 \pm 6 \times 10^{-16} *$	$-0.13991 \pm 7 \times 10^{-16} *$
$Sr_{n+1}Ti_nO_{3n+1}$ (298K)	4	2	1–3,∞	0.37907 ± 0.00085	-0.01143 ± 0.00097
$Sr_{n+1}Zr_nO_{3n+1}$ (298K)	4	2	1–3,∞	0.34264 ± 0.00028	-0.0056 ± 0.0003
$La_{n+1}Ni_nO_{3n+1}$ (298K)	4	2	1–3,∞	0.69749 ± 0.0015	-0.01505 ± 0.00169

* extremely small value of standard error results from insufficient number of experimental points ($N = 3$) and degrees of freedom ($df = 1$).

It is noteworthy that no significant correlation was found between B_1 and B_2 coefficients at $p < 0.05$ (Pearson's correlation coefficient 0.0736, Spearman rank order correlation $\rho = 0.2619$). We can therefore treat the terms B_1/n and B_2/n^2 as independent and ascribe to them a reasonable, simple physical interpretation. It seems that there are at least three main factors that could potentially influence the stability of the $AO(ABO_3)_n$ phase structure. These factors could be (i) the nature of the parent perovskite ABO_3 , (ii) the dimensionality of the perovskite block n , and (iii) the modulation of the crystal structure by AO layers. Thus,

the term $G_{n/P} = (\Delta G_{1/n}/\Delta G_P - 1)$ in Equation (10) is related to the thermodynamics of the parent perovskite ABO_3 and corresponds to the relative excess of the molar Gibbs energy of the RP phase $(AO)_{1/n}ABO_3$ compared to that of ABO_3 . The term B_1/n reflects the additive properties of the structure and accounts for the progressive decrease in the contribution of the insertion of the AO layer to the Gibbs energy with increasing dimension n of the perovskite block. The negative non-linear term B_2/n^2 corresponds to the contribution to the stabilization of the structure. This can be attributed to the interaction of the layers of rock salt with each other.

The present paper does not aim to define the exact physical meaning of B coefficients. Instead, it introduces the conception of performing thermodynamic analysis using the reciprocal value of n . At this stage, the coefficients B_1 and B_2 are empirical fitting parameters and are determined from experimental data. Further development of Equation (10) may involve a theoretical or semi-empirical evaluation of these coefficients, which will allow the calculation of the Gibbs free energy values. Figure 3 clearly shows the obvious correlation between the coefficient B_1 and Goldschmidt's tolerance factor (TF_{per}), which provides evidence that such assessments are possible. This dependence is quite logical, as TF_{per} is an indicator for the stability and distortion of perovskite structures, and, as mentioned above, the coefficient B_1 can be related to the dimensionality of the perovskite block. The relationship of the B_2 coefficient and specific physical and chemical characteristics is more problematic. However, the theoretical calculation of these parameters is beyond the scope of this paper and is the subject of future research.

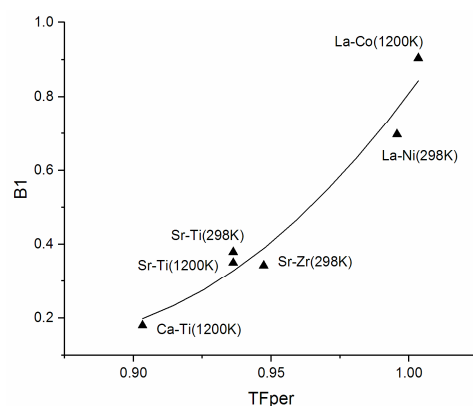


Figure 3. Values of fitted B_1 parameter plotted against the respective tolerance factor (TF_{per}) of ABO_3 perovskite. The tolerance factor is derived from 12 coordination number radii of A ions [29]. The solid line is a guide to the eye.

4. Conclusions

The proposed dependence (5) permits for the calculation of the molar Gibbs energies of the formation of the Ruddlesden–Popper phases $(AO)_{1/n}ABO_3$, wherein the reciprocal value of the index n is employed as a variable. The calculation is based on the molar Gibbs energy of formation of the parent perovskite ABO_3 and incorporates two supplementary empirical parameters.

This dependence (5) can be transformed into a dimensionless Equation (10), which, when employed, translates the experimental points into a set of analogous curves that pass through the origin. In this case, the first parameter (B_1) is responsible for the slope of the curve, and the second (B_2) determines its curvature. While the exact physical interpretation of B_1 and B_2 parameters is currently unclear, it is reasonable to assume that the first one is associated with the description of the additive changes in Gibbs energy with an increase in the perovskite block dimension, while the second (non-linear) relates to stabilization of the layered structure.

We believe that the approach associated with the description of the thermodynamic properties of RP phases in the space of reciprocal values of the index n is promising for the search of the most general regularities, which will yield an extensive set of possibilities for

thermodynamic prediction within and across layered perovskite-like RP phases, and possibly can be extended to other layered perovskites (Aurivillius and Dion–Jacobson phases).

Author Contributions: Conceptualization, S.V.; methodology, S.V.; writing—original draft preparation, S.V. and V.D.; writing—review and editing, S.V.; formal analysis, V.D.; data curation, V.D. All authors have read and agreed to the published version of the manuscript.

Funding: This research received no external funding.

Data Availability Statement: No new data were created or analyzed in this study.

Acknowledgments: The work was carried out within the framework of the state assignment of the Institute of Chemistry and Chemical Technology of the Siberian Branch of the Russian Academy of Sciences (project FWES 2021-0013).

Conflicts of Interest: The authors declare no conflict of interest.

References

1. Tilley, R.J.D. *Perovskites: Structure–Property Relationships*; Wiley & Sons Ltd.: Hoboken, NJ, USA, 2016.
2. Samreen, A.; Ali, M.S.; Huzaifa, M.; Ali, N.; Hassan, B.; Ullah, F.; Ali, S.; Arifin, N.A. Advancements in Perovskite-Based Cathode Materials for Solid Oxide Fuel Cells: A Comprehensive Review. *Chem. Rec.* **2024**, *1*, e202300247. [\[CrossRef\]](#) [\[PubMed\]](#)
3. Wang, Q.; Fan, H.; Xiao, Y.; Zhang, Y. Applications and recent advances of rare earth in solid oxide fuel cells. *J. Rare Earths* **2022**, *40*, 1668–1681. [\[CrossRef\]](#)
4. Han, N.; Shen, Z.; Zhao, X.; Chen, R.; Thakur, V.K. Perovskite oxides for oxygen transport: Chemistry and material horizons. *Sci. Total Environ.* **2022**, *806*, 151213. [\[CrossRef\]](#) [\[PubMed\]](#)
5. Zhang, M.; Jeerh, G.; Zou, P.; Lan, R.; Wang, M.; Wang, H.; Tao, S. Recent development of perovskite oxide-based electrocatalysts and their applications in low to intermediate temperature electrochemical devices. *Mater. Today* **2021**, *49*, 351–377. [\[CrossRef\]](#)
6. Xu, X.; Pan, Y.; Zhong, Y.; Ran, R.; Shao, Z. Ruddlesden–Popper perovskites in electrocatalysis. *Mater. Horizons* **2020**, *7*, 2519–2565. [\[CrossRef\]](#)
7. Xu, X.; Pan, Y.; Ge, L.; Chen, Y.; Mao, X.; Guan, D.; Li, M.; Zhong, Y.; Hu, Z.; Peterson, V.K.; et al. High-Performance Perovskite Composite Electrocatalysts Enabled by Controllable Interface Engineering. *Small* **2021**, *17*, 2101573. [\[CrossRef\]](#)
8. Noguera, C. Theoretical investigation of the Ruddlesden–Popper compounds $\text{Sr}_{n+1}\text{TiO}_{3n+1}$ ($n = 1–3$). *Philos. Mag. Lett.* **2000**, *80*, 173–180. [\[CrossRef\]](#)
9. Ludt, C.; Zschornak, M. Electronic structure of the homologous series of Ruddlesden–Popper phases $\text{SrO}(\text{SrTiO}_3)_n$, ($n = 0–3, \infty$). *Zeitschrift für Krist.–Cryst. Mater.* **2022**, *237*, 201–214. [\[CrossRef\]](#)
10. McCARTHY, G.J.; White, W.B.; Roy, R. Phase Equilibria in the 1375 °C Isotherm of the System Sr–Ti–O. *J. Am. Ceram. Soc.* **1969**, *52*, 463–467. [\[CrossRef\]](#)
11. Carleschi, E.; Doyle, B.P.; Fittipaldi, R.; Granata, V.; Strydom, A.M.; Cuoco, M.; Vecchione, A. Double metamagnetic transition in $\text{Sr}_4\text{Ru}_3\text{O}_{10}$. *Phys. Rev. B* **2014**, *90*, 205120. [\[CrossRef\]](#)
12. Banerjee, A.; Prasad, R.; Venugopal, V. Thermodynamic properties of $\text{Sr}_2\text{RuO}_4(\text{s})$ and $\text{Sr}_3\text{Ru}_2\text{O}_7(\text{s})$ by using solid–state electrochemical cells. *J. Alloys Compd.* **2004**, *373*, 59–66. [\[CrossRef\]](#)
13. Elcombe, M.M.; Kisi, E.H.; Hawkins, K.D.; White, T.J.; Goodman, P.; Matheson, S. Structure determinations for $\text{Ca}_3\text{Ti}_2\text{O}_7$, $\text{Ca}_4\text{Ti}_3\text{O}_{10}$, $\text{Ca}_{3.6}\text{Sr}_{0.4}\text{Ti}_3\text{O}_{10}$ and a refinement of $\text{Sr}_3\text{Ti}_2\text{O}_7$. *Acta Crystallogr. Sect. B Struct. Sci.* **1991**, *47*, 305–314. [\[CrossRef\]](#)
14. Ram, R.M.; Ganapathi, L.; Ganguly, P.; Rao, C.N.R. Evolution of three–dimensional character across the $\text{La}_{n+1}\text{NiO}_{3n+1}$ homologous series with increase in n. *J. Solid State Chem.* **1986**, *63*, 139–147. [\[CrossRef\]](#)
15. Zinkevich, M.; Solak, N.; Nitsche, H.; Ahrens, M.; Aldinger, F. Stability and thermodynamic functions of lanthanum nickelates. *J. Alloys Compd.* **2007**, *438*, 92–99. [\[CrossRef\]](#)
16. Yan, L.; Niu, H.J.; Duong, G.V.; Suchomel, M.R.; Bacs, J.; Chalker, P.R.; Hadermann, J.; Van Tendeloo, G.; Rosseinsky, M.J. Cation ordering within the perovskite block of a six–layer Ruddlesden–Popper oxide from layer–by–layer growth—Artificial interfaces in complex unit cells. *Chem. Sci.* **2011**, *2*, 261–272. [\[CrossRef\]](#)
17. Lee, C.H.; Podraza, N.J.; Zhu, Y.; Berger, R.F.; Shen, S.; Sestak, M.; Collins, R.W.; Kourkoutis, L.F.; Mundy, J.A.; Wang, H.; et al. Effect of reduced dimensionality on the optical band gap of SrTiO_3 . *Appl. Phys. Lett.* **2013**, *102*, 122901. [\[CrossRef\]](#)
18. Barone, M.R.; Dawley, N.M.; Nair, H.P.; Goodge, B.H.; Holtz, M.E.; Soukiasian, A.; Fleck, E.E.; Lee, K.; Jia, Y.; Heeg, T.; et al. Improved control of atomic layering in perovskite–related homologous series. *APL Mater.* **2021**, *9*, 021118. [\[CrossRef\]](#)
19. Yokokawa, H.; Sakai, N.; Kawada, T.; Dokiya, M. Thermodynamic stability of perovskites and related compounds in some alkaline earth–transition metal–oxygen systems. *J. Solid State Chem.* **1991**, *94*, 106–120. [\[CrossRef\]](#)
20. Glasser, L. Systematic Thermodynamics of Layered Perovskites: Ruddlesden–Popper Phases. *Inorg. Chem.* **2017**, *56*, 8920–8925. [\[CrossRef\]](#)
21. Bannikov, D.O.; Safronov, A.P.; Cherepanov, V.A. Thermochemical characteristics of $\text{La}_{n+1}\text{NiO}_{3n+1}$ oxides. *Thermochim. Acta* **2006**, *451*, 22–26. [\[CrossRef\]](#)

22. Jacob, K.T.; Rajitha, G. Thermodynamic properties of strontium titanates: Sr_2TiO_4 , $\text{Sr}_3\text{Ti}_2\text{O}_7$, $\text{Sr}_4\text{Ti}_3\text{O}_{10}$, and SrTiO_3 . *J. Chem. Thermodyn.* **2011**, *43*, 51–57. [\[CrossRef\]](#)
23. Jacob, K.T.; Abraham, K.P. Thermodynamic properties of calcium titanates: CaTiO_3 , $\text{Ca}_4\text{Ti}_3\text{O}_{10}$, and $\text{Ca}_3\text{Ti}_2\text{O}_7$. *J. Chem. Thermodyn.* **2009**, *41*, 816–820. [\[CrossRef\]](#)
24. Parida, S.C.; Singh, Z.; Dash, S.; Prasad, R.; Venugopal, V. Standard molar Gibbs energies of formation of the ternary compounds in the La–Co–O system using solid oxide galvanic cell method. *J. Alloys Compd.* **1999**, *285*, 7–11. [\[CrossRef\]](#)
25. Petrov, A.N.; Cherepanov, V.A.; Zuyev, A.Y.; Zhukovsky, V.M. Thermodynamic stability of ternary oxides in LnMO ($\text{Ln} = \text{La, Pr, Nd}$; $\text{M} = \text{Co, Ni, Cu}$) systems. *J. Solid State Chem.* **1988**, *77*, 1–14. [\[CrossRef\]](#)
26. Bannikov, D.O.; Cherepanov, V.A. Thermodynamic properties of complex oxides in the La–Ni–O system. *J. Solid State Chem.* **2006**, *179*, 2721–2727. [\[CrossRef\]](#)
27. Ao, X.; Zhu, L.; Liang, R.; Wang, Y.; Ye, M.; Zheng, R.; Ke, S. Phase transition from SrRuO_3 to $\text{Sr}_3\text{Ru}_2\text{O}_7$ by tuning oxygen pressure at low processing temperature. *Scr. Mater.* **2024**, *238*, 115745. [\[CrossRef\]](#)
28. Vereshchagin, S.N.; Budnikov, V.A.; Nasluzov, V.A.; Solovyov, L.A. Synthesis and Stability of Ruddlesden–Popper Phases $(\text{Sr}_{0.8}\text{Ln}_{0.2})_3\text{Co}_2\text{O}_{7-\delta}$ ($\text{Ln} = \text{Sm, Gd, Dy}$). *J. Sib. Fed. Univ. Chem* **2024**, *17*, 279–288.
29. Shannon, R.D. Revised effective ionic radii and systematic studies of interatomic distances in halides and chalcogenides. *Acta Crystallogr. Sect. A* **1976**, *32*, 751–767. [\[CrossRef\]](#)

Disclaimer/Publisher’s Note: The statements, opinions and data contained in all publications are solely those of the individual author(s) and contributor(s) and not of MDPI and/or the editor(s). MDPI and/or the editor(s) disclaim responsibility for any injury to people or property resulting from any ideas, methods, instructions or products referred to in the content.